Solution of the kinetic equation for the deposited energy distribution in the power cross section model

1994 J. Phys.: Condens. Matter 6 4181

(http://iopscience.iop.org/0953-8984/6/22/017)

J. Phys.: Condens. Matter 6 (1994) 4181–4196. Printed in the UK

Solution of the kinetic equation for the deposited energy distribution in the power cross section model

L G Glazov
High Current Electronics Institute, Akademichesky 4, Tomsk, Russia

Received 9 December 1993, in final form 22 March 1994

Abstract. A regular method for finding solutions of the equation for the distribution of energy deposited by atomic particles in elastic collisions is developed, using the model of an infinite random medium and power cross section. It is shown that in neglecting threshold energy the distribution derivative has a singularity at the target surface. The calculated distributions and other functions connected with the problem are given for the case of equal masses of the projectile and target atoms.

1. Introduction

The present paper is devoted to a new investigation of the classical problem of finding the deposited energy distributions for interactions between ions and amorphous or polycrystalline targets in the linear cascade model [1, 2]. Following a pioneer paper [1] and a series of later papers [3–6], we adopt the simplest correct analytical model of the phenomenon: (i) an infinite isotropic random medium, (ii) a power cross section of elastic collisions, (iii) neglect of electronic energy losses, and (iv) threshold energy [1].

The well known results of solving this problem need to be revised for the following reason. It is known that in the adopted model the system of equations for the spatial moments of the distribution F_D to be found is easily solved, and the problem of constructing a good approximation to the distribution F_D from a finite number of moments arises [1, 3, 7–10]. However, no respective regular procedure was found for the function F_D, because all the methods so far used do not provide good convergence (see, for instance, [1, 8]); the termination of summing a series, or a recurrent procedure, is not based on any physical or mathematical arguments. From the mathematical point of view, this situation arises because the function F_D is not differentiable, as will be shown below. Therefore, smooth function expansions for F_D cannot be quickly convergent. Let us introduce the Fourier transform $f_D(k)$ of the function $F_D(z)$. The function $f_D(k)$ decreases too slowly ($\sim k^{-\alpha}$ with $\alpha \leqslant 2$) at large k because, in particular, the derivative of $F_D(z)$ has a singularity at $z = 0$. This fact (i) provides a relatively high dependence of $F_D(z)$ on the wing of $f_D(k)$, particularly for values of $F_D(z)$ close to the target surface $z = 0$; (ii) makes questionable the approximations for $F_D(z)$ by functions of which the Fourier transforms decrease too quickly (for example, exponentially) when $k \to \infty$; and (iii) makes incorrect the methods of finding $f_D(k)$ for all k, when only a few first derivatives at $k = 0$ are known (i.e. constructing some approximation for $F_D(z)$ from a few first spatial moments).

An ignorance of all these factors creates a danger of a non-predictable error when building F_D by usual methods. This is also reflected in Monte Carlo simulation methods. Although Monte Carlo methods generally do not depend on moments analyses, the

0953-8984/94/224181+16$19.50

usual analytical approach nevertheless leads to a choice of differentiable functions for approximation of the numerical results, and gives estimates that are too low for the number of tests necessary for a correct description of the deposited energy distribution behaviour near the target surface.

In this paper we suggest a regular and dependable method of solving the kinetic equation for the deposited energy distributions in the boundaries of the above-described model. For simplicity, we discuss only the case of equal masses of an ion and a target atom.

2. The method of solving the kinetic equation

2.1. The kinetic equation for the deposited energy distribution

The initial equation can be easily derived by the linear cascade theory, and in the adopted model can be written in the form [1]

$$-\eta\frac{\partial F_D(z,E,\eta)}{\partial z}=\frac{N}{2\pi}\int_0^E\frac{d\sigma(E,T)}{dT}\,dT\int de'\{\delta(e\cdot e'-\sqrt{1-T/E})\times[F_D(z,E,\eta)-F_D(z,E-T,\eta')]-\delta(e\cdot e'-\sqrt{T/E})F_D(z,T,\eta')\}. \quad (1)$$

Here N is the density of the target atoms; e, e' are the unit vectors in the direction of the starting and scattering (or recoiling) particle velocities; $\eta=\cos\theta$, $\eta'=\cos\theta'$ are the respective direction cosines, i.e. $e\cdot e'=\cos\theta\cos\theta'-\sin\theta\sin\theta'\cos\varphi'$, $de'=\sin\theta'\,d\theta'\,d\varphi'$; $F_D(z,E,\eta)$ is the deposited energy distribution to be found: $F_D(z,E,\eta)\,dz$ is the average energy, deposited in the coordinate interval $(z,z+dz)$ during the development of the cascade caused by one projectile starting at the plane $z=0$ with energy E, $\eta=\cos\theta$ being the direction cosine of initial velocity with respect to the z axis; and $d\sigma(E,T)$ is the differential (on recoil energy T) cross section of elastic collisions; further, we use the power cross section [1, 2, 6]

$$d\sigma(E,T)=CE^{-m}T^{-1-m}\,dT \quad (2)$$

where $m=$ constant is the parameter of the power cross section, $0<m<1$, C is a constant depending on the type of the target and the selected value of m; furthermore, when investigating the asymptotic behaviour of the solution we examine the case $\frac{1}{3}\leqslant m\leqslant\frac{1}{2}$.

Equation (1) and the energy conservation condition

$$\int_{-\infty}^{\infty}F_D(z,E,\eta)\,dz=E \quad (3)$$

define the function to be found.

The function $F_D(z,E,\eta)$ can be represented in the following form:

$$F_D(z,E,\eta)=NCE^{1-2m}F(zNC/E^{2m},\eta) \quad (4)$$

where F is a function of dimensionless variables. The possibility of the representation (4) can be proved using the well known fact that the nth spatial moment of the function F_D is proportional to E^{1+2mn} [1]. The representation (4) can also be checked by inserting (4) into (1).

Introducing new dimensionless variables $x = zNC/E^{2m}$ and $t = T/E$ we obtain the equation determining the function $F(x, \eta)$:

$$-\eta\frac{\partial F(x,\eta)}{\partial x} = \frac{1}{2\pi}\int_0^1 t^{-1-m}\,dt\int de'\{\delta(e\cdot e' - \sqrt{1-t}) \times [F(x,\eta) - (1-t)^{1-2m}F(x/(1-t)^{2m},\eta')] - \delta(e\cdot e' - \sqrt{t})t^{1-2m}F(x/t^{2m},\eta')\} \tag{5}$$

and the condition

$$\int_{-\infty}^{\infty} F(x,\eta)\,dx = 1. \tag{6}$$

2.2. Legendre polynomials expansion

The function $F(x, \eta)$ can be expanded in terms of Legendre polynomials:

$$F(x,\eta) = \sum_{l=0}^{\infty}(2l+1)P_l(\eta)F_l(x). \tag{7}$$

The coefficient functions F_l satisfy the following system of equations ($l = 0, 1, 2, \ldots, F_{-1} \equiv 0$):

$$-\frac{\partial}{\partial x}[lF_{l-1}(x) + (l+1)F_{l+1}(x)] = (2l+1)\int_0^1 t^{-1-m}\,dt \times [F_l(x) - P_l(\sqrt{1-t})(1-t)^{1-2m}F_l(x/(1-t)^{2m}) - P_l(\sqrt{t})t^{1-2m}F_l(x/t^{2m})]. \tag{8}$$

For the functions F_l, $l \geqslant 0$ the condition (6) is

$$\int_{-\infty}^{\infty} F_l(x)\,dx = \delta_{l0}. \tag{9}$$

The functions $F_l(x)$ with even and odd l are symmetric and antisymmetric respectively.

2.3. Equations for the Fourier transforms

We introduce the Fourier transform of the function $F(x, \eta)$:

$$F(x,\eta) = \frac{1}{2\pi}\int_{-\infty}^{\infty} e^{ikx} f(k,\eta)\,dk \tag{10}$$

$$f(k,\eta) = \int_{-\infty}^{\infty} e^{-ikx}F(x,\eta)\,dx. \tag{11}$$

The function $f(k, \eta)$ also can be expanded in terms of Legendre polynomials:

$$f(k,\eta) = \sum_{l=0}^{\infty}(2l+1)P_l(\eta)f_l(k). \tag{12}$$

The functions F_l and f_l are related by formulae similar to (10) and (11).

The system (8) leads to a system of equations for the functions $f_l(k)$, $f_{-1} \equiv 0$:

$$-ik[lf_{l-1}(k) + (l+1)f_{l+1}(k)] = (2l+1)\int_0^1 t^{-1-m}\,dt \times \left[f_l(k) - P_l\left(\sqrt{1-t}\right)(1-t)f_l(k(1-t)^{2m}) - P_l(\sqrt{t})tf_l(kt^{2m})\right]. \tag{13}$$

The formulae (9) give the boundary conditions for the equations (13):

$$f_l(0) = \delta_{l0}. \tag{14}$$

The functions $f_{2l}(k)$ are real and symmetric functions of k, $f_{2l+1}(k)$ being imaginary and antisymmetric.

We note here an interesting numerical observation: each function $f_l(k)$ does not change sign in the region $k > 0$ as far as it was tabulated in the present work, and $f_l > 0$ for $l = 0, 4, 8, \ldots$, $f_l < 0$ for $l = 2, 6, 10, \ldots$, $\mathrm{Im} f_l < 0$ for $l = 1, 5, 9, \ldots$, $\mathrm{Im} f_l > 0$ for $l = 3, 7, 11, \ldots$. It takes place at least for $l \leqslant 30$, $m = 1/2$ and $1/3$, $k \leqslant 30$ and $k \leqslant 12$ respectively. Unfortunately, attempts to prove a general statement of this kind were not successful.

2.4. Recurrence relations for the spatial moments

Let us introduce the spatial moments of the functions $F(x, \eta)$, $F_l(x)$:

$$F^n(\eta) = \int_{-\infty}^{\infty} x^n F(x, \eta)\,dx \qquad n = 0, 1, 2, \ldots \tag{15}$$

$$F_l^n = \int_{-\infty}^{\infty} x^n F_l(x)\,dx \qquad n = 0, 1, 2, \ldots \tag{16}$$

$$F^n(\eta) = \sum_{l=0}^{\infty} (2l+1)P_l(\eta)F_l^n \qquad n = 0, 1, 2, \ldots. \tag{17}$$

The equations (8) give recurrence relations for calculating F_l^n [1]:

$$F_l^n = \frac{n[lF_{l-1}^{n-1} + (l+1)F_{l+1}^{n-1}]}{(2l+1)I_l(1+2mn)} \qquad l \leqslant n,\ n \geqslant 1. \tag{18}$$

Here

$$I_l(s) = \int_0^1 t^{-1-m}\,dt\left[1 - P_l(\sqrt{1-t})(1-t)^s - P_l(\sqrt{t})t^s\right] = -\frac{1}{m} - (-1)^{[l/2]}\frac{(l/2 - [l/2] - s + m + 1/2)_{[l/2]}}{(l/2 - [l/2] + s - m)_{[l/2]+1}} - 2^{-l}\sum_{p=0}^{[l/2]}(-1)^p C_l^p C_{2l-2p}^l B(-m, s + l/2 - p + 1) \tag{19}$$

where $(a)_k = \Gamma(a+k)/\Gamma(a)$, $[a]$ is an integer part of a, $B(x, y)$ is a beta function, and $C_l^p = l!/p!(l-p)!$.

The formulae (18) provide the possibility of calculating the moments of the distribution F recursively, with the conditions (9) as starting values:

$$F_l^0 = \delta_{l0}. \tag{20}$$

2.5. *The series for the Fourier transform*

Knowing the moments F_l^n one can tabulate the Fourier transform $f(k, \eta)$:

$$f(k, \eta) = \sum_{n=0}^{\infty} (-ik)^n F^n(\eta)/n!. \tag{21}$$

A method based upon the Taylor expansion for the Fourier transform was previously used in a series of papers [11–13] dealing with constructing different damage cascade distributions (the energy and momentum deposition profiles and the net recoil density respectively) from the spatial moments. By constructing Padé approximants to the Taylor series, the authors of these papers obtained sequences of approximate expressions for the Fourier transform, for which the inverse transformation can be performed analytically. In the present paper we are going to use a more direct method based upon immediate tabulation of the Taylor series and the following continuation of the Fourier transform in accordance with analytically established asymptotic expressions. The moments and the terms in the series (21) ought to be calculated with the maximum available precision to reach as high a value of k as possible directly tabulating $f(k)$.

2.6. *Symmetric and antisymmetric parts of the functions*

The function $f(k, \eta)$ can be represented in the form

$$f(k, \eta) = f_S(k, \eta) + i f_A(k, \eta). \tag{22}$$

The real part f_S is a symmetric function of both k and η, is determined by moments with even n, and contains only the terms with even l in the Legendre polynomial expansion.

The imaginary part f_A is an antisymmetric function of both k and η (and, respectively, it is equal to zero for $\eta = 0$), is determined by moments with odd n, and contains only the terms with odd l in the Legendre polynomial expansion.

The functions f_S and f_A determine the symmetric and antisymmetric parts of the distribution $F(x, \eta)$ respectively:

$$F(x, \eta) = F_S(x, \eta) + F_A(x, \eta) \tag{23}$$

$$F_S(-x, \eta) = F_S(x, \eta) \qquad F_S(x, -\eta) = F_S(x, \eta)$$

$$F_A(-x, \eta) = -F_A(x, \eta) \qquad F_A(x, -\eta) = -F_A(x, \eta)$$

$$F_S(x, \eta) = \frac{1}{\pi} \int_0^{\infty} \cos(kx) f_S(k, \eta)\, dk \tag{24a}$$

$$F_A(x, \eta) = -\frac{1}{\pi} \int_0^{\infty} \sin(kx) f_A(k, \eta)\, dk. \tag{24b}$$

2.7. The asymptotic behaviour of the functions for the cases $k \to \infty$ and $x \to 0$

By calculating the moments and tabulating the series (21), one can obtain $f(k, \eta)$ up to some value $k = k_0$. Usually one can reach values for $f(k, \eta)$ of the order of a few per cent of the maximum by this method. One then has to make the correct continuation of the Fourier transform in the region $k > k_0$. The precision of this continuation is not very important for determining values of $F(x, \eta)$ (being found by tabulating (10)) far away from the point $x = 0$, because $\partial f(k)/\partial k$ decreases much faster than $f(k)$; but it is critical for an adequate calculation of $F(x, \eta)$ in the case $x \approx 0$.

The function $f(k, \eta)$ very slowly decreases when $k \to \infty$; in particular, the function $F(x, \eta)$ is not differentiable at $x = 0$. For example, it is easy to show directly from (8) that for odd l and $m \geqslant 1/3$

$$\left.\frac{\partial F_l(x)}{\partial x}\right|_{x=0} = \infty.$$

It is therefore necessary to investigate the asymptotes of the function to be found at $k \to \infty$ and $x \to 0$ for the correct continuation of the Fourier transform in the region $k > k_0$, and for an understanding of the characteristic features of the behaviour of $F(x, \eta)$ near the target surface.

Note here that the opposite-case asymptotes, i.e. the large-depth decrease of the damage profile, were investigated in [14].

2.7.1. The case $m = \frac{1}{2}$. The $x \to 0$ asymptotes. In the case $m = \frac{1}{2}$ equations (8) are

$$-\frac{\partial}{\partial x}[lF_{l-1}(x) + (l+1)F_{l+1}(x)] = (2l+1)\int_0^1 t^{-3/2}\,dt \times \left[F_l(x) - P_l\left(\sqrt{1-t}\right)F_l\left(x/(1-t)\right) - P_l\left(\sqrt{t}\right)F_l(x/t)\right].$$

When $x \to 0$, the last term on the right-hand side appears to be the leading one. Let us examine the case $l = 0$, $x \to +0$:

$$-\frac{\partial F_1(x)}{\partial x} \sim -\int_0^1 t^{-3/2}F_0(x/t)\,dt = -x^{-1/2}\int_x^\infty \xi^{-1/2}F_0(\xi)\,d\xi$$
$$= -x^{-1/2}\int_0^\infty \xi^{-1/2}F_0(\xi)\,d\xi + x^{-1/2}\int_0^x \xi^{-1/2}F_0(\xi)\,d\xi$$
$$= \text{constant} \times x^{-1/2} + \text{constant} + \ldots.$$

The function $F_1(x)$ is antisymmetric, $F_1(0) = 0$, and when $x \to +0$

$$F_1(x) \sim \text{constant} \times x^{1/2} + \text{constant} \times x + \ldots$$

and antisymmetrically for $x < 0$.

In the same way, for $l = 1$, $x \to +0$ we obtain

$$\frac{\partial}{\partial x}[F_0(x) + 2F_2(x)] \sim 3\int_0^1 t^{-1}F_1(x/t)\,dt = 3\int_x^\infty \xi^{-1}F_1(\xi)\,d\xi$$
$$= 3\int_0^\infty \xi^{-1}F_1(\xi)\,d\xi - 3\int_0^x \xi^{-1}F_1(\xi)\,d\xi.$$

The first integral on the right-hand side is finite, because $F_1(\xi) \sim \xi^{1/2}$. So when $x \to +0$

$$\frac{\partial}{\partial x}[F_0(x) + 2F_2(x)] \sim \text{constant} + \text{constant} \times x^{1/2} + \dots$$

and taking into account the symmetry of the functions F_{2l}, we obtain

$$F_0(x) + 2F_2(x) \sim \text{constant} + \text{constant} \times |x| + \text{constant} \times |x|^{3/2} + \dots \qquad |x| \to 0.$$

These formulae can be easily extended on all functions with odd and even l respectively. Therefore the antisymmetric functions $F_{2l+1} \sim \sqrt{x}$ near the target surface, their derivatives at $x = 0$ being infinite; the derivative of any symmetric function F_{2l} abruptly changes sign at $x = 0$.

2.7.2. The case $m = \frac{1}{2}$. The $k \to \infty$ asymptotes. In the case $m = 1/2$ equations (13) become

$$-ik\left[lf_{l-1}(k) + (l+1)f_{l+1}(k)\right] = (2l+1)\int_0^1 t^{-3/2}\,dt \times \left[f_l(k) - P_l\left(\sqrt{1-t}\right)(1-t)f_l(k(1-t)) - P_l\left(\sqrt{t}\right)tf_l(kt)\right].$$

When $k \to \infty$, the last term on the right-hand side appears to be the leading one. Let us examine the case $l = 0$, $k \to +\infty$:

$$-ikf_1(k) \sim -\int_0^1 t^{-1/2} f_0(kt)\,dt = -k^{-1/2}\int_0^k \xi^{-1/2} f_0(\xi)\,d\xi = -k^{-1/2}\int_0^\infty \xi^{-1/2} f_0(\xi)\,d\xi + k^{-1/2}\int_k^\infty \xi^{-1/2} f_0(\xi)\,d\xi.$$

We therefore obtain

$$f_1(k) \sim \text{constant} \times k^{-3/2} + \dots \qquad k \to +\infty$$

and antisymmetrically for $k \to -\infty$.

For $l = 1$, $k \to +\infty$:

$$ik[f_0(k) + 2f_0(k)] \sim 3\int_0^1 f_1(kt)\,dt = 3k^{-1}\int_0^k f_1(\xi)\,d\xi = 3k^{-1}\int_0^\infty f_1(\xi)\,d\xi - 3k^{-1}\int_k^\infty f_1(\xi)\,d\xi$$

and taking into account the symmetry of the functions $f_l(k)$ with even l:

$$f_0(k) + 2f_2(k) \sim \text{constant} \times |k|^{-2} + \text{constant} \times |k|^{-5/2} \qquad |k| \to \infty.$$

These formulae can be easily extended on all functions with odd and even l respectively. So the antisymmetric functions $f_{2l+1} \sim k^{-3/2}$ when $k \to +\infty$; the symmetric functions $f_{2l} \sim \text{constant} \times |k|^{-2} + \text{constant} \times |k|^{-5/2}$ when $k \to \infty$.

2.7.3. The asymptotes for $\frac{1}{3} \leqslant m \leqslant \frac{1}{2}$. For other values of m the asymptotic forms of the functions at $x \to 0$ and $k \to \infty$ can be investigated by the same method, although the formulae are more complicated. The respective results are given below.

For the functions with odd l at $x \to +0$:

$$F_l(x) \sim \text{constant} \times x^{1/2m-1/2} + \text{constant} \times x + \ldots \qquad 1/3 < m \leqslant 1/2$$
$$F_l(x) \sim \text{constant} \times x \ln x + \text{constant} \times x + \ldots \qquad m = 1/3$$

and for the functions with odd l at $k \to +\infty$:

$$f_l(k) \sim \text{constant} \times k^{-1/2-1/2m} + \ldots \qquad 1/3 \leqslant m \leqslant 1/2$$

and antisymmetrically for $x \to -0$ and $k \to -\infty$.

For the functions with even l at $x \to +0$:

$$F_l(x) \sim \text{constant} + \text{constant} \times x^{3/4m-1/2} + \text{constant} \times x^{1/2m+1/2} + \ldots \qquad 1/3 < m \leqslant 1/2$$
$$F_l(x) \sim \text{constant} + \text{constant} \times x^{7/4} + \text{constant} \times x^2 \ln x + \text{constant} \times x^2 + \ldots \qquad m = 1/3$$

and for the functions with even l at $k \to +\infty$:

$$f_l(k) \sim \text{constant} \times k^{-1/2-3/4m} + \text{constant} \times k^{-1/2m-3/2} + \ldots \qquad 1/3 \leqslant m \leqslant 1/2$$

and symmetrically for $x \to -0$ and $k \to -\infty$.

It is necessary to note that the singularity of $\partial F(x, \eta)/\partial x$ at $x = 0$ is caused by neglecting threshold energy.

We thus have dealt with the special case of the singularity at the target surface. It is not a new problem. The problem of the discontinuity at the surface has been extensively discussed in the literature on electron slowing and energy deposition. The pertinent profiles were found by Monte Carlo simulation as early as the 1950s. A discontinuity at the surface was formally introduced in [11] for calculating the damage profile in the large ion-to-target-atom mass-ratio case. Another type of discontinuity was discussed in [13], devoted to determining the net recoil density, which has an $x^{-1/2}$ singularity at the target surface. These papers used modifications of the Padé approximants method for constructing distributions with a fixed discontinuity.

2.8. The procedure for solving the kinetic equation

The following procedure was used for solving the kinetic equation. According to the recurrence formulae (18) the moments of the distribution were calculated with the maximum available precision (when using 28-decimal- digit precision it is usually enough to calculate the moments up to $n = 300$); the function $f(k, \eta)$ and a few of its first derivatives were then tabulated using (21) up to some value $k = k_0$, where the series can be found with enough accuracy. Further, the Fourier transform was continued in the region $k > k_0$ independently for real and imaginary parts of $f(k, \eta)$ by determining constants in asymptotic formulae from the condition of the best coincidence near the point $k = k_0$. The symmetric and antisymmetric parts of the function to be found were calculated by formulae (24). The accuracy of the results was controlled by using different methods for determining the asymptotic expansion coefficients and checking the condition of almost full mutual compensation of the contributions of symmetric and antisymmetric parts of the distribution at large-enough negative x. Except in the small region $x \approx 0$ the relative error is of the order of 0.1%. A method for a more accurate calculation of $F(x = 0, \eta)$ is discussed below.

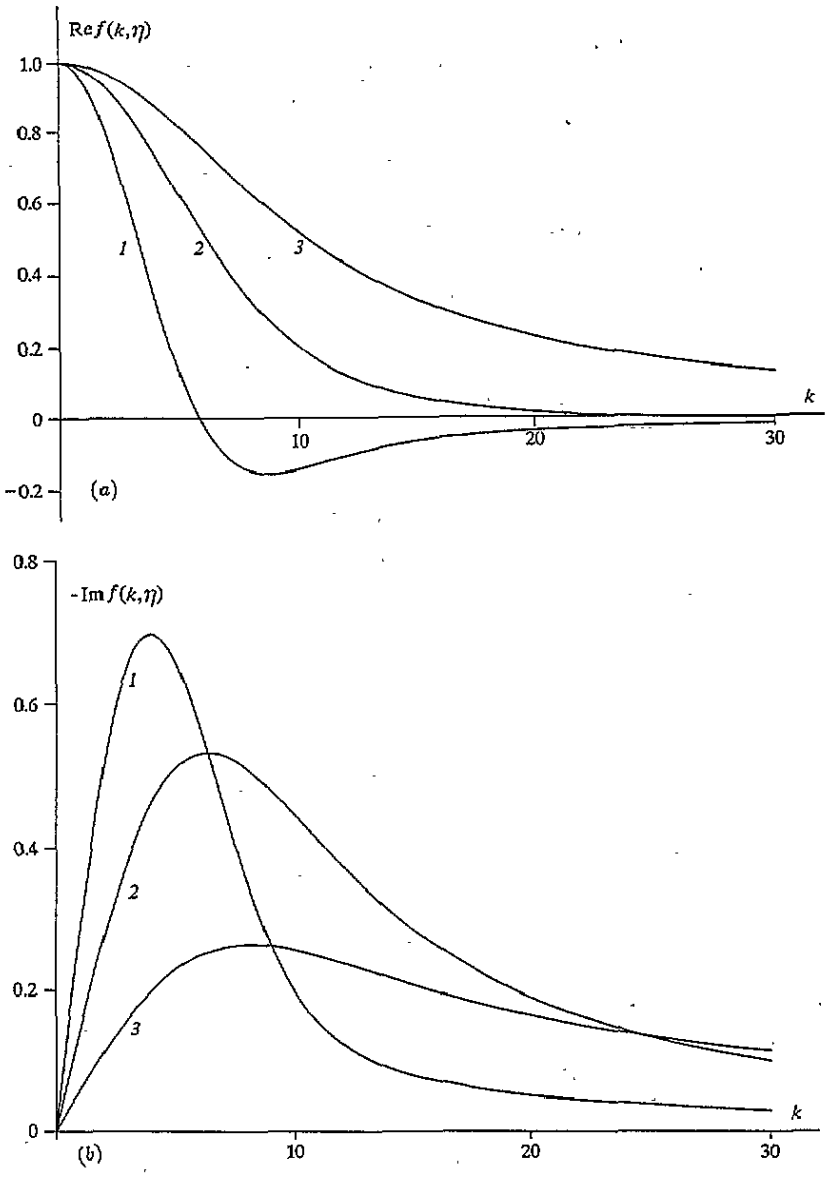

Figure 1. Dependence of the real (a) and imaginary (b) (with inverse sign) parts of the Fourier transform $f(k, \eta)$ on k; $m = 1/2$; $\eta = 1$ (1), $\eta = 0.5$ (2), $\eta = 0.2$ (3).

3. Results

Figure 1(a) and (b) demonstrates the characteristic behaviour of the Fourier transforms Ref and Imf, which have been obtained by tabulating the series (21). The smaller η, the higher the curve Re$f(k, \eta)$ becomes, and it provides an increase in the value $F(x = 0, \eta)$. At $\eta \approx 1$ the direct tabulation of the series (21) gives a possibility of reaching values Re$f(k, \eta) \sim 0.02$, but the regions of positive and negative values of Re$f(k, \eta)$ strongly compensate each other when calculating $F(x = 0, \eta)$. It causes a relatively high dependence of the $F(x = 0, \eta)$ calculation precision on the accuracy of the Re$f(k, \eta)$ continuation in

the region $k > k_0$.

The behaviour of the zeroth and first angular harmonics of the distribution for $m = 1/2$ as a function of the coordinate is shown in figure 2. According to general features of the asymptotic behaviour of the functions at $x \to 0$, the function $F_1(x)$ has an infinite derivative and the derivative of the function $F_0(x)$ abruptly changes sign at $x = 0$.

Figure 3 shows the characteristic symmetric and antisymmetric parts of the distribution. For large-enough negative x they compensate each other with good precision, providing small values of the distribution. Taking into account the independence of finding asymptotes for their Fourier transforms, it is an additional confirmation of the good accuracy of the obtained results.

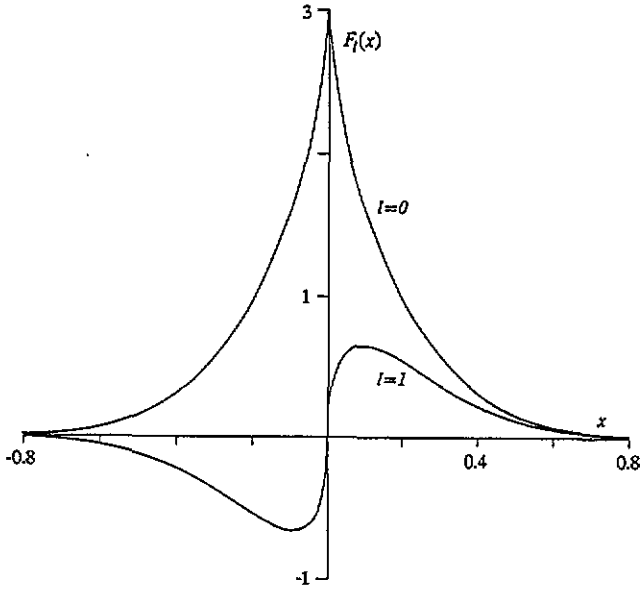

Figure 2. Dependences $F_0(x)$ and $F_1(x)$; $m = 1/2$.

Figure 4 demonstrates the functions $F(x, \eta)$ for normal ($\eta = 1$) and tangential ($\eta = 0$) incidence of an ion for $m = 1/2$. The results for $\eta = 0$ cannot be appropriate because in this case the model of an infinite medium does not provide a correct description of the phenomenon. However, these results are of definite interest from the mathematical point of view, because in this case the antisymmetric part of $F(x, \eta)$ disappears, and $F(x, \eta = 0)$ demonstrates a behavior that is typical for symmetric functions of the problem for $m = 1/2$: its derivative abruptly changes sign at $x = 0$ and the function is characterized by Λ-like behaviour near the target surface. Furthermore, $F(x, \eta = 0)$ can be considered as the deposited energy distribution in the perpendicular direction for normal incidence. One can easily see that in this case any quasi-normal approximations are incorrect.

The approximations with an exponentially decreasing Fourier transform were mentioned above to lead to badly convergent series or recurrent procedures. For comparison with the results of the present paper, the author tried Gram–Charlie, Edgeworth series and similar

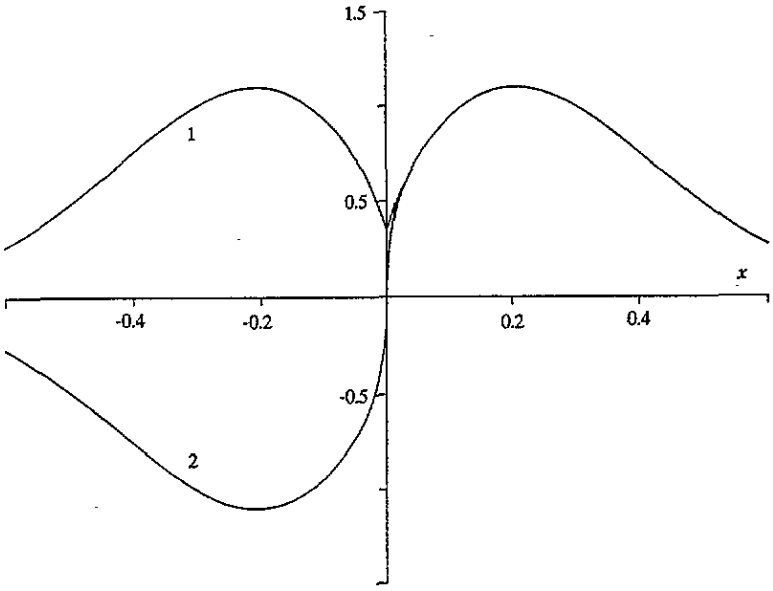

Figure 3. Symmetric (1) and antisymmetric (2) parts of $F(x, \eta = 1)$; $m = 1/2$.

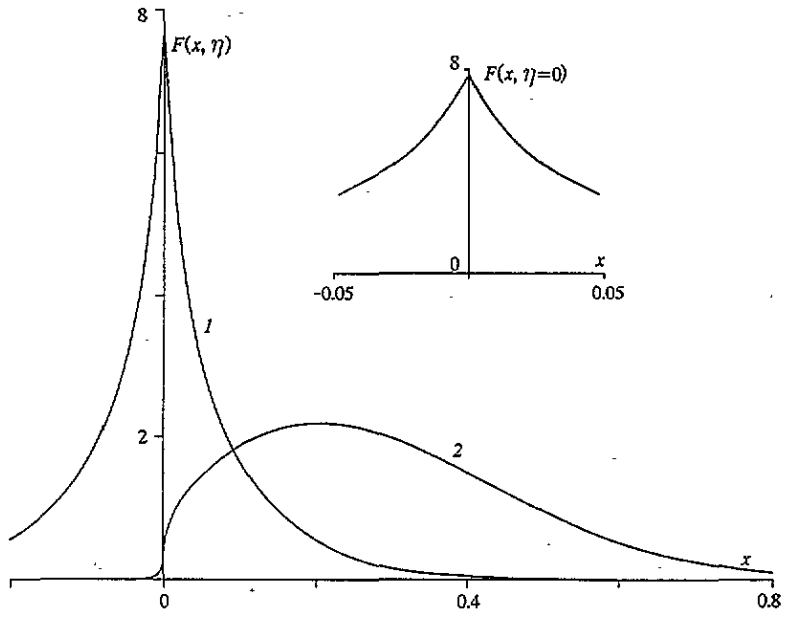

Figure 4. Dependences $F(x, \eta)$ for tangential and normal incidence; $m = 1/2$; $\eta = 0$ (1), $\eta = 1$ (2).

methods, which are described in detail in [1], wherein $\leqslant 20$ terms were taken into account and it gave qualitatively correct profiles (except for the singularity in the derivative, of course). Having high-precision data on the moments of the distribution, one can tabulate with enough accuracy at least several hundred terms in series of this kind. However, these

methods clearly appear to be not regular: beginning from some critical number of terms n_{cr} taken into account, the sum quickly becomes an oscillating function and cannot be a reasonable approximation. As a rule, n_{cr} strongly decreases with decreasing η. For example, for usual Gram–Charlie series $n_{cr} \sim 50--100$ for $\eta = 1$ and $n_{cr} \sim 10--20$ for $\eta = 1/2$. Some Gram–Charlie curves for $m = 1/2$, $\eta = 1$ are shown in figure 5 for comparison.

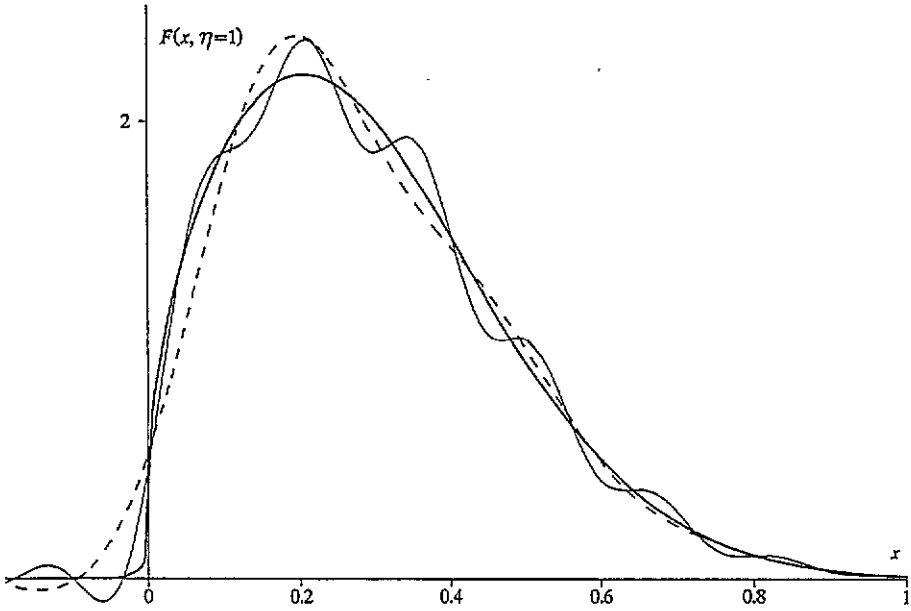

Figure 5. $F(x, \eta = 1)$ for $m = 1/2$ (thick full curve) and respective Gram–Charlie expansion curves with 10 (broken curve) and 50 (thin full curve) moments taken into account (the algorithm of calculating coefficients is described in detail in appendix B of [1]).

Finally, figure 6(*a*) and (*b*) shows the curves $F(x, \eta)$ for $m = 1/2$ and $m = 1/3$ respectively. All the curves are characterized by a rapid change in the function near the surface and an infinite derivative at $x = 0$.

4. Calculating $F(x = 0, \beta)$

The method of calculating $F(x, \eta)$ described above gives a precise result except, perhaps, for a small region near the surface $x = 0$. The following circumstances make less accurate the calculation of $F(x = 0, \eta)$ by Fourier transformation inversion. (i) The Fourier transform slowly decreases when $k \to \infty$, so the value of $F(x = 0, \eta)$ strongly depends upon the accuracy of the selection of asymptotes. (ii) A very rapid change in $F(x, \eta)$ near the surface creates difficulties for correct numerical calculation. (iii) For small η the function $f(k, \eta)$ reaches a desired asymptote at too large a value of k. In contrast, in the case $\eta \approx 1$, $f_S(k, \eta)$ quickly reaches the desired asymptote, but due to the strong mutual compensation of the regions of positive and negative values of f_S, one needs too high an accuracy of the selection of the asymptotic expansion coefficients. (iv) The accuracy of finding asymptotic formulae for f_S (determining $F(x = 0)$) is much worse than for f_A. This is connected with

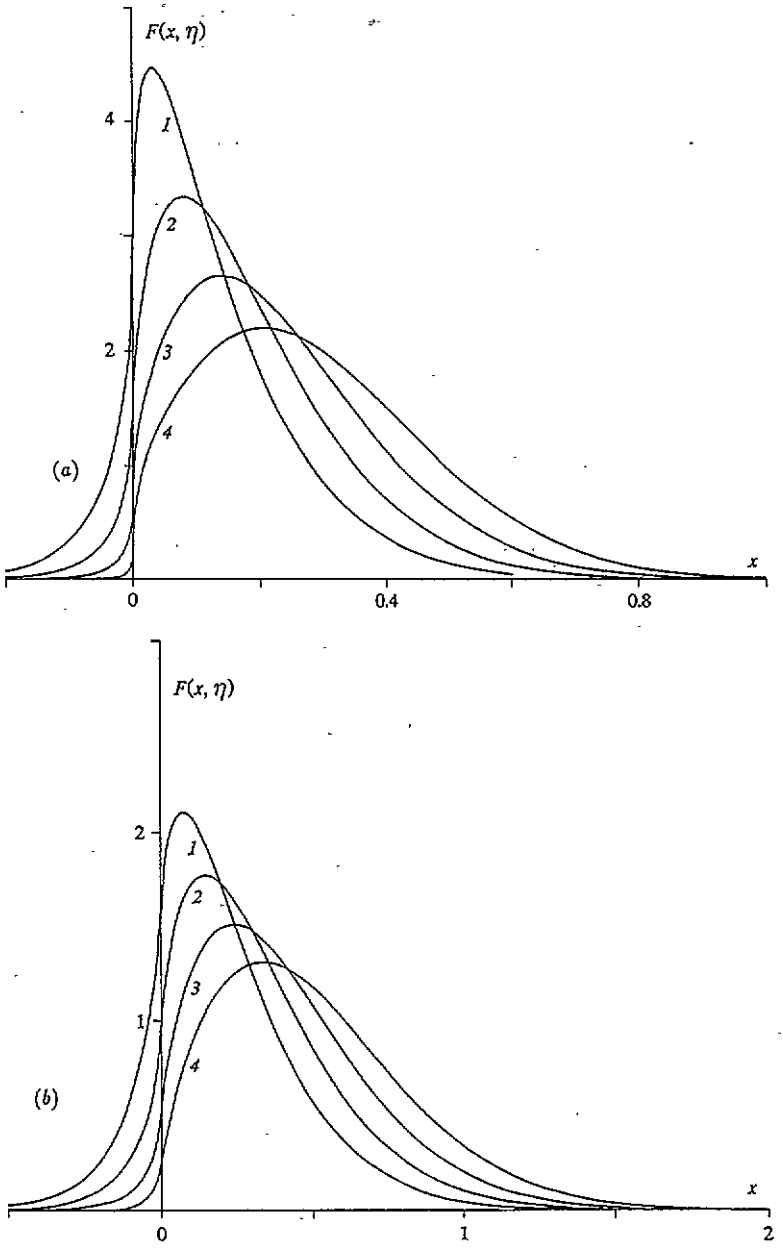

Figure 6. Dependences $F(x, \eta)$ on x for $m = 1/2$ (*a*) and $m = 1/3$ (*b*); $\eta = 0.4$ (1), $\eta = 0.6$ (2), $\eta = 0.8$ (3), $\eta = 1$ (4).

the fact that symmetric function expansions have two leading terms with similar powers of k ($\sim k^{-2}$, $\sim k^{-5/2}$ at $m = 1/2$; $\sim k^{-11/4}$, $\sim k^{-3}$ at $m = 1/3$), which usually strongly compensate each other. So it would be more correct to express $F(x = 0, \eta)$ in terms of some antisymmetric functions of the problem.

These circumstances can provide a relative error of the order of 20% when calculating $F(x = 0, \eta)$, if the spatial moments are tabulated with a precision of 16–28 decimal digits.

Although it is not too much compared with the general change in $F(x,\eta)$ in the surface region, it sharply contrasts with the high precision in determining $F(x,\eta)$ at other points. On the other hand, a correct calculation of $F(x,\eta)$ is very important due to well known applications in sputtering theory, and so on. It is therefore necessary to build an independent method of calculating $F(x=0,\eta)$, which ought to be free of the defects mentioned above.

Integrating the system of equations (8), we obtain

$$lF_{l-1}(0)+(l+1)F_{l+1}(0)=(2l+1)\int_0^\infty F_l(x)\,dx$$
$$\times\int_0^1 t^{-1-m}\,dt\left[1-P_l\left(\sqrt{1-t}\right)(1-t)-P_l\left(\sqrt{t}\right)t\right]$$
$$(2l+1)I_l(1)=\int_0^\infty F_l(x)\,dx$$

and, after multiplying by $P_l(\eta)$ and summing over l:

$$\eta F(x=0,\eta)=\sum{}'(2l+1)P_l(\eta)I_l(1)\int_0^\infty F_l(x)\,dx.$$

The sum on the right-hand side includes only the terms with odd l. Formally it is provided by the fact that $I_0(1)=0$ and for even $l>0$

$$\int_0^\infty F_l(x)\,dx=\frac{1}{2}\int_{-\infty}^\infty F_l(x)\,dx=0$$

according to the condition (9).

Let us introduce the function

$$\Psi(x,\eta)=\sum_{l=1,3,\ldots}(2l+1)P_l(\eta)I_l(1)F_l(x).$$

Its Fourier transform

$$\psi(k,\eta)=\sum_{l=1,3,\ldots}(2l+1)P_l(\eta)I_l(1)f_l(k)$$

is an imaginary and antisymmetric function of k, $\psi(0,\eta)=0$, so one can write

$$\int_0^\infty\Psi(x,\eta)\,dx=\frac{1}{2\pi}\int_0^\infty dx\int_{-\infty}^\infty e^{ikx}\psi(k,\eta)\,dk=-\frac{1}{\pi}\int_0^\infty k^{-1}\,\mathrm{Im}\,\psi(k,\eta)\,dk.$$

In this way we obtain the following formula for $F(x=0,\eta)$:

$$F(x=0,\eta)=-\frac{1}{\pi\eta}\int_0^\infty k^{-1}\,\mathrm{Im}\,\psi(k,\eta)\,dk. \tag{25}$$

The tabulation of $\psi(k,\eta)$ at $k<k_0$ can be reduced (according to (21)) to summing a series

$$\mathrm{Im}\,\psi(k,\eta)=-\sum_{n=0}^\infty\frac{(-1)^nk^{2n+1}}{(2n+1)!}\sum_{l=1,3,\ldots}(2l+1)P_l(\eta)I_l(1)F_l^{2n+1}. \tag{26}$$

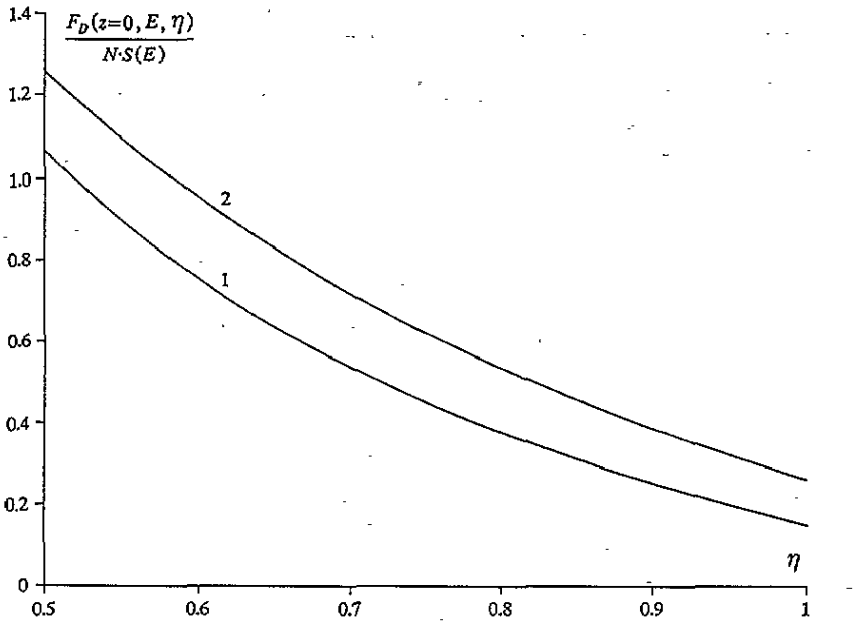

Figure 7. $F_D(z=0, E, \eta)/NS(E)$ for $m = 1/2$ (1) and $m = 1/3$ (2).

The continuation on the region $k > k_0$ can be made by the same method as for other antisymmetric functions of the problem.

Use of (25) and (26) for calculating $F(x = 0, \eta)$ provides the following advantages. (i) The region $k > k_0$ gives a small contribution into the integral (25) due to a faster decrease at large k of the function being integrated, than when calculating Fourier transformation inversion. Respectively, the error connected with uncertainties in asymptotic expansion coefficients becomes smaller. (ii) Continuation in the region $k > k_0$ is made for the antisymmetric function $\psi(k, \eta)$; it also provides better accuracy.

Figure 7 demonstrates the curves

$$F_D(z = 0, E, \eta)/NS(E) = (1 - m)F(x = 0, \eta)$$

for $1/2 \leqslant \eta \leqslant 1$ and $m = 1/2, 1/3$,

$$S(E) = \int T \, d\sigma = E^{2m}/(1 - m)NC$$

being the stopping power; the relative error is not higher than about 1%.

5. Conclusion

A regular method has been proposed for solving the kinetic equation for the spatial distribution of energy deposited in a collision cascade caused by a projectile ion in an amorphous or polycrystalline target. The model of an infinite medium and power cross section of elastic collisions is used for a description of the phenomenon. The method is based upon finding the Fourier transform of the distribution and provides the possibility of

obtaining a kinetic equation solution with arbitrary accuracy. The results of tabulating the deposited energy distribution and other characteristic functions connected with the problem have been presented for the case of equal masses of the projectile ion and target atoms.

The asymptotic behaviour of different functions connected with the problem has been investigated. It has been shown, in particular, that in neglecting a threshold energy, the derivative of the distribution has a singularity at the target surface for $m \geqslant 1/3$. It makes incorrect the usual methods of finding the distribution based on constructing a smooth approximation from a few first spatial moments. The solution obtained demonstrates a very fast change near the target surface.

A special method of calculating the value of the distribution at the target surface has been examined. The method provides higher accuracy for fixed precision of tabulating spatial moments. The respective results have been given.

References

[1] Winterbon K B, Sigmund P and Sanders J B 1970 *Mat. Fys. Medd. Dan. Vid. Selsk.* **37** No 14
[2] Sigmund P 1969 *Phys. Rev.* **184** 383
[3] Winterbon K B 1975 *Ion Implantation Depth and Deposited Energy Distributions* (New York: Plenum)
[4] Sigmund P 1977 *Inelastic Ion–Surface Collisions* ed N H Tolk *et al* (New York: Academic) p 121
[5] Sigmund P 1987 *Nucl. Instrum. Methods* B **27** 1
[6] Falcone D 1990 *Rev. Nuovo Cimento* **13** 1
[7] Sigmund P 1968 *Can. J. Phys.* **46** 731
[8] Winterbon K B 1972 *Rad. Effects* **13** 215
[9] Winterbon K B 1976 *Rad. Effects* **30** 199
[10] Brice D K 1970 *Rad. Effects* **6** 77; 1974 *J. Nucl. Mater.* **53** 213; 1975 *J. Appl. Phys.* **46** 3385
[11] Littmark U and Maderlechner G 1976 *Proc. SPIG* p 139
[12] Littmark U and Sigmund P 1975 *J. Phys. D: Appl. Phys.* **8** 241
[13] Winterbon K B 1980 *Rad. Effects* **46** 181
[14] Winterbon K B 1972 *Rad. Effects* **15** 73